

Thermal Degradation Rate and Kinetic Modeling of CO₂-Loaded Amine Solvent Blends of 2-Amino-2-methyl-1-propanol and 1-Amino-2-propanol

Naser S. Matin,[†] Jesse Thompson,^{†,‡} Keemia Abad,^{†,‡} Saloni Bhatnagar,[†] and Kunlei Liu^{*,†,§,¶}

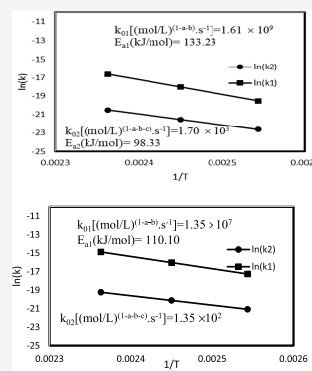
[†]Center for Applied Energy Research, University of Kentucky, 2540 Research Park Drive, Lexington, Kentucky 40511, United States

[‡]Department of Chemistry, University of Kentucky, Lexington, Kentucky 40506, United States

[§]Department of Mechanical Engineering, University of Kentucky, Lexington, Kentucky 40506, United States

Supporting Information

ABSTRACT: Power-law rate equations for the thermal degradation of 1-amino-2-propanol (A2P) and 2-amino-2-methyl-1-propanol (AMP) in CO₂-loaded blended solutions are determined with the experimental kinetic data collected in this study. The rate experiments were conducted at 120, 135, and 150 °C to accelerate thermal degradation. The kinetic data collected were used to obtain the initial rate equation from blended solutions of 0.0, 0.5, 1.5, 2.0, 2.5, and 3.5 M, AMP and A2P with CO₂ loadings from 0.1 to 0.6, mol_{CO₂}/mol_{AMP+A2P}. The power-law rate equations for each amine in the solutions, along with pre-exponential factors and activation energies for each reaction are provided. For both AMP and A2P degradation, the activation energies for the reaction between AMP, A2P, and CO₂ presented lower values, while the pre-exponential factors were orders of magnitude higher. The presence of the second amine in these solutions has little impact on the degradation rate of the individual amines.



1. INTRODUCTION

Employing blends of aqueous alkanolamine solutions for postcombustion CO₂ absorption is a practical choice to take advantage of the individual solvent characteristics.^{1–3} Because of the practical advantages of aqueous solutions of mixed alkanolamines, including primary, secondary, tertiary, and hindered amines, for acid gas (e.g., carbon dioxide) separations, their equilibrium properties are widely investigated.^{4–14} Blends of amine solutions can have synergistically beneficial effects from each component during the CO₂ absorption and regeneration process. While primary and secondary amines generally exhibit a high CO₂ absorption rate, the high heat of regeneration, and low achievable CO₂ loading (mol of CO₂ captured/mol of amine), tertiary amines show the opposite behavior with relatively low reactivity and low heat of regeneration. However, the development and selection of new solvents and, consequently, the design of improved capture processes are the primary targets for much current research work related to CO₂ capture. To obtain beneficial synergistic effects, blended amines have been investigated for absorbing CO₂, for example, blended monoethanolamine (MEA) and methyldiethanolamine (MDEA); piperazine (PZ) and MDEA; AMP (2-amino-2-methyl-1-propanol) and PZ; diethanolamine (DEA) and AMP; triethanolamine (TEA)/AMP/MDEA; DEA/MEA/PZ; MEA and 4-(diethylamino)-2-butanol (DEAB); and DEA/MDEA/AMP.^{13,15–22} Solutions of blended amines offer a way to obtain a high-performance solvent with higher CO₂ cyclic capacity, targeted energy of regeneration, and higher absorption kinetics.

Because of their structure, sterically hindered (primary or secondary) amines are often used in such blends to take advantage of their relatively high absorption rates and high achievable CO₂ loadings. A sterically hindered amine is defined as either a primary amine in which the amino group is attached to a tertiary carbon or a secondary amine in which the amino group is attached to at least one secondary or tertiary carbon.²³ The steric hindrance structure leads to unstable carbamate species and a bicarbonate pathway. Sterically hindered amines also generally have low volatilities and low degradation rates as a consequence of the bicarbonate reaction pathway.

AMP is an example of hindered amine as a hindered form of MEA displaying lower carbamate stability, better loading capacity for CO₂, especially at higher pressures, and a higher equilibrium temperature sensitivity when compared to MEA.^{18,24,25} As to the importance of the corrosion in aqueous alkanolamine solutions, it has also been shown that the sterically hindered amines have much lower corrosion rates than their unhindered forms.^{26,27} However, the desirable properties associated with steric hindrance are offset by the slow CO₂ absorption rate in alkanolamine solutions.²⁴ A2P is a primary amine with a bulky, isopropanol group that increases solubility in aqueous solutions. The isopropyl group is also associated with slightly slower CO₂ absorption kinetics

Received: September 26, 2019

Revised: December 13, 2019

Accepted: December 16, 2019

Published: December 16, 2019

compared to MEA.²⁸ Compared to other alkanolamines such as MDEA, 3-amino-1-propanol (AP), TEA, DEA, and MEA, both A2P and AMP have higher surface activities, which will have a positive impact on the mass transfer at the gas–liquid interface.^{29,30} The abovementioned properties for AMP and A2P make them potentially valuable for use as CO₂ capture solvents either as an individual component solvent, or more interestingly as candidates for blending into a combined solvent. However, not all amines are compatible when blended together, especially related to their degradation profile. The presence of a second amine in the solvent has been shown to catalyze and enhance the thermal degradation of the main amine component.³¹

AMP can be prone to degradation at high temperatures, despite its perception as generally being resistant to degradation.^{32,33} Previous studies have shown that AMP can form a carbamate (AMPCOO⁻) with CO₂ leading to thermal degradation with a similar pathway to that of MEA.^{32,34–36} The thermal degradation rate of AMP to its main degradation product, 4,4-dimethyl-1,3-oxazolidin-2-one (DMOZD), was investigated in detail by considering an apparent reaction rate and pseudo-mechanistic approach.^{36,37} The previous work introduced an inclusive apparent power-law AMP and CO₂ concentration-dependent reaction rate for AMP degradation to DMOZD in a broad range of AMP and CO₂ concentrations and system temperature. In the current study, the previous rate equation and parameters introduced for the AMP degradation rate in its CO₂ aqueous solutions are considered, along with the effect of the second chemical component in the reaction rate.

The thermal degradation rates and the effect of each amine within the blended solvent on the other amine degradation rate were investigated over a broad range of amine concentrations and at relevant stripper temperatures between 120 and 150 °C. The solutions, their preparation, experimental rate data gathering, and data analysis are discussed. The finalized reaction rates are shown as the amine degradation rates as a function of both amines and CO₂ concentration. Finally, the rate equations for the degradation of both amines, along with rate model parameters, including the pre-exponential factor and activation energy, are provided.

2. EXPERIMENTAL SECTION

2.1. Amine Solution Preparation. The initial bulk 2-amino-2-methyl-1-propanol (AMP; Acros Organics) and 1-amino-2-propanol (A2P; Sigma-Aldrich) solutions were prepared to the target carbon dioxide content.³² Table 1 shows the composition of each amine in the solutions, along with the total CO₂ loading. The solvent test matrix is composed of seven different combinations of AMP and A2P at CO₂-rich loading conditions, along with four equal composition blends at four different CO₂-loadings from lean to rich. This set allows for the determination of the impact of each individual component and CO₂-loading.

2.2. Thermal Degradation. Thermal degradation experiments were performed in stainless steel tubes using a previously reported method.³² Sample tubes were maintained at 120, 135, and 150 °C and removed after 8, 48, and 96 h. The sample tubes were weighed, opened, and transferred to vials before analysis. Tubes having greater than 1.5% weight change were excluded from the data set.

2.3. Method of Analysis. Degradation products were identified and quantified by HPLC-TOF-MS using the

Table 1. Amine Solvent Blends and CO₂-Loading Used for Thermal Degradation Experiments

solution	AMP (mol/L)	A2P (mol/L)	CO ₂ loading (mol _{CO₂} /mol amine)
1	0.0	3.5	0.6
2	0.5	3.5	0.6
3	1.5	3.5	0.6
4	2.0	3.5	0.6
5	3.5	0.5	0.6
6	3.5	1.5	0.6
7	3.5	2.0	0.6
8	2.5	2.5	0.1
9	2.5	2.5	0.2
10	2.5	2.5	0.4
11	2.5	2.5	0.6

methodology described previously.^{32,38} Identification and quantification of the primary degradation product from AMP, DMOZD, was performed according to the methodology described by Matin et al. (2016). Identification of A2P degradation products was performed using a methodology similar to that described by Thompson et al. (2017) by calculating the mass accuracy of the observed mass spectral peaks and the resulting molecular formula and comparing this to anticipated thermal degradation products for primary alkanolamines with CO₂.³⁸

Authentic degradation compounds used for calibration and quantification were purchased for DMOZD, MeOZD, N-(2-hydroxyethyl)ethylenediamine (HEEDA), N-(2-hydroxyethyl)imidazolidin-2-one (HEIA), and 1-(2-hydroxyethyl)imidazole (HEI) from Sigma-Aldrich (St. Louis, MO). When an authentic standard of a degradation compound was not available, a representative calibration curve was applied on the basis of structural similarity to calculate the concentration.^{38,39} In this study, HEIA was used for 1-(2-hydroxypropyl)-5-methyl-2-imidazolidinone (HPMZD); HEEDA was used for 1-[(2-amino-1-methylethyl)amino]-2-propanol (AMEA2P); and HEI was used for N,N'-bis(2-hydroxypropyl)urea quantification.

3. RESULTS AND DISCUSSION

3.1. Experimental Thermal Degradation. The primary thermal degradation reaction for AMP is shown in Figure 1,^{32,36} proceeding through amine-carbamate formation with

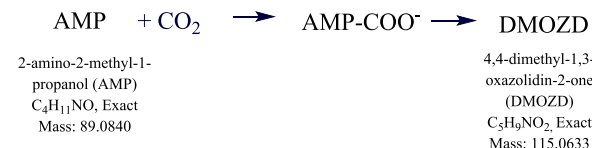


Figure 1. Primary AMP thermal degradation pathway (Matin et al. 2017).

CO₂, followed by an intermolecular cyclization/dehydration step to produce the cyclic degradation product DMOZD. The degradation pathway for A2P was derived in this study using the reported degradation pathway for similar primary alkanolamines, including monoethanolamine (MEA), and the degradation reactions proposed by Gouédard (2014).⁴⁰ The proposed thermal degradation pathway for A2P is presented in Figure 2. Similar to MEA and AMP, thermal degradation in the presence of CO₂ is the result of a reaction involving the A2P-

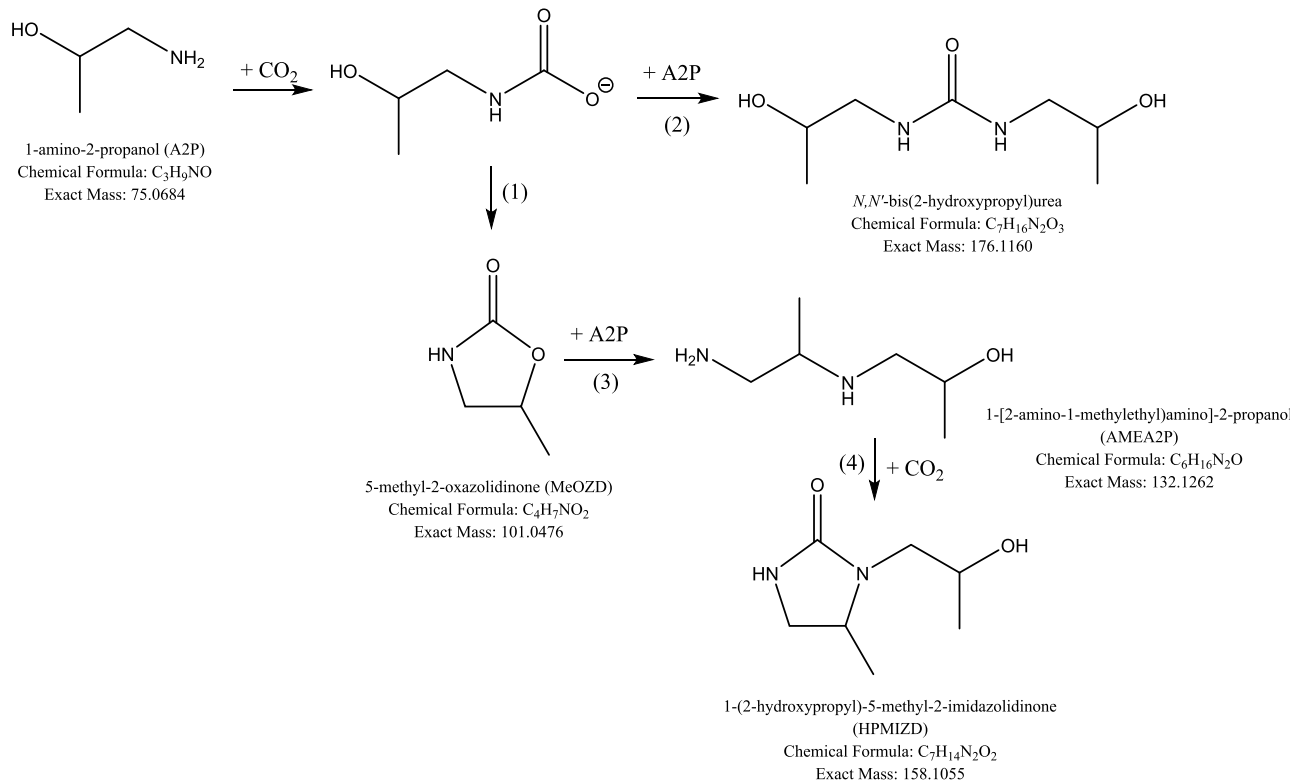


Figure 2. Proposed A2P thermal degradation pathway.

carbamate. This carbamate can either undergo an intermolecular cyclization/dehydration reaction to form the cyclic MeOZD (1) or can be subjected to nucleophilic attack by free (unreacted) A2P, yielding *N,N'*-bis(2-hydroxypropyl)urea (2). While the urea compound is stable and does not undergo further reactions within the timeframe and temperature range of this study, the cyclic oxazolidinone compound can be considered to be relatively unstable and can undergo a subsequent reaction with another free A2P (3) to form 1-[2-amino-1-methylethyl]amino]-2-propanol (AMEA2P).³² This reaction has a direct corollary with MEA as it undergoes the identical reaction to form *N*-(2-hydroxyethyl)ethylenediamine (HEEDA).³⁸ The final reaction observed in this study (4) involves AMEA2P-carbamate formation (reaction with CO₂) followed by a second intermolecular cyclization/dehydration reaction to form the cyclic 1-(2-hydroxypropyl)-5-methyl-2-imidazolidinone (HPMIZD). This reaction also occurs with MEA in the formation of HEIA.

In this work, to be consistent with the previous published kinetic model for AMP, the DMOZD formation rate is considered to be equal to the AMP degradation rate.^{36,37} However, in the case of A2P, because of different amine degradation products and the potential for parallel reactions, the same assumption could not be made. Therefore, the A2P degradation rate is determined and reported in this study.

Figures 3–5 display the DMOZD formation as a function of time at different A2P concentrations and temperatures (solutions #2–4 in Table 1) with constant AMP concentration (3.5 M) and constant CO₂-loading. The corresponding plots for the DMOZD concentration versus time at 120, 135, and 150 °C, and different AMP and A2P concentrations and CO₂ loadings are presented in Figures S1–S6 in the Supporting Information. The A2P concentration changes do not have meaningful effects on the DMOZD formation, while the AMP

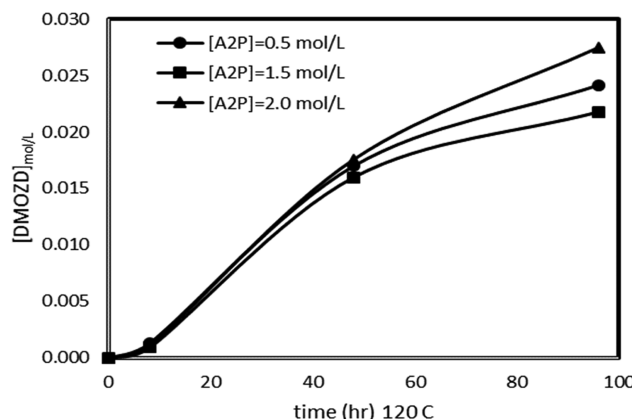


Figure 3. DMOZD concentration as a function of time (CO₂ loading of 0.6 (mol_{CO₂}/mol_{AMP+A2P}), and [AMP] = 3.5 M, at 120 °C).

concentration, temperature, and CO₂ loading does have a noticeable impact on DMOZD formation (Figures S1–S6). As expected, higher CO₂ loading and higher temperature lead to higher degradation for AMP. The DMOZD formation at 120 and 135 °C is ascending over time, with no obvious maximum point at the end time of the experiment. While at 150 °C, DMOZD appears to be approaching a relatively flat region after an approximate maximum point of [DMOZD] = 0.14 M, at CO₂ loading of 0.6 mol_{CO₂}/mol_{total amine}, and [AMP] = 3.5 M (Figure 5). This behavior is consistent with previous observation in aqueous solutions of only AMP.³⁷

The approach for the DMOZD formation rate measurement was described in our previous work.³⁷ The mass spectroscopic analysis confirmed that at the initial stages of the reaction, DMOZD is the only AMP degradation product.³⁷

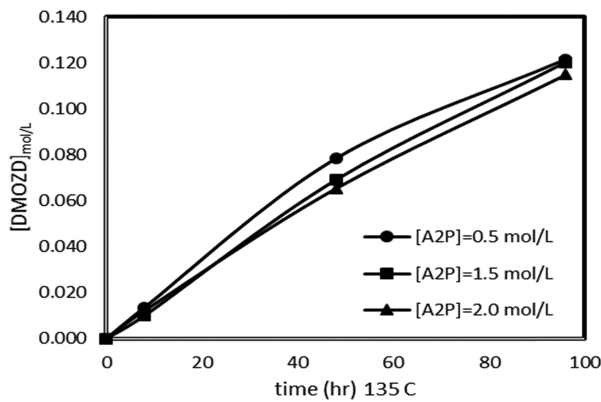


Figure 4. DMOZD concentration as a function of time (CO_2 loading of 0.6 ($\text{mol}_{\text{CO}_2}/\text{mol}_{\text{AMP}+\text{A2P}}$), and $[\text{AMP}] = 3.5 \text{ M}$, at 135°C).

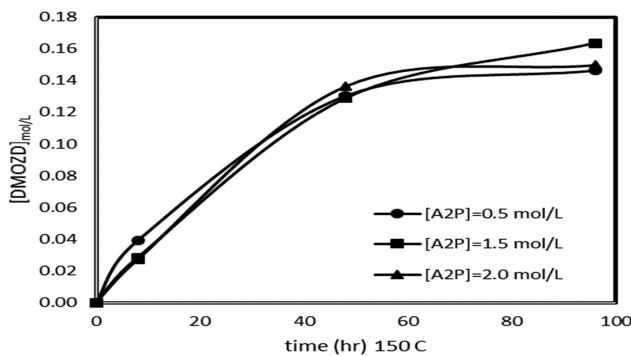


Figure 5. DMOZD concentration as a function of time (CO_2 loading of 0.6 ($\text{mol}_{\text{CO}_2}/\text{mol}_{\text{AMP}+\text{A2P}}$), and $[\text{AMP}] = 3.5 \text{ M}$, at 150°C).

The A2P degradation as a function of time at different A2P concentrations and two limiting temperatures, 120 and 150°C (solution #5–7), is shown in Figure 6, with no significant

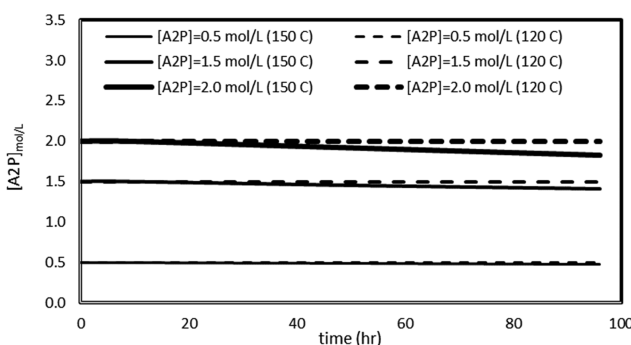


Figure 6. A2P concentration as a function of time (CO_2 loading of 0.6 ($\text{mol}_{\text{CO}_2}/\text{mol}_{\text{AMP}+\text{A2P}}$), and $[\text{AMP}] = 3.5 \text{ M}$, at 120 and 150°C).

changes in A2P concentration observed, particularly at low temperatures and low A2P concentrations. The corresponding plots for the change of the A2P concentration versus time at 120, 135, and 150°C , and at varying AMP concentrations and CO_2 loadings are presented in Figures S7–S12 in the Supporting Information. As with the very negligible effect of the presence of A2P on the AMP degradation, likewise, the presence of AMP does not have a noticeable impact on the A2P degradation. Also, similar is the fact that the A2P concentration and CO_2 loading have an appreciable impact on the A2P degradation. In these blended aqueous solutions,

neither of the amines has a meaningful impact on the degradation of the other amine. Nevertheless, in the case of both amines, degradation increases with solution loading and temperature and with AMP and A2P concentrations.

When assuming DMOZD as the sole degradation product of AMP in the time interval used in this study, A2P as a nonhindered alkanolamine is more susceptible to degradation than AMP, Figures S1–S3 compared to S4–S6. The A2P degradation in the solution causes a significant drop in active amine concentration from 2.5 M to around 1.6 M, at 150°C , and at CO_2 loadings equal or higher than 0.6 $\text{mol}_{\text{CO}_2}/\text{mol}_{\text{total amine}}$, Figures S10–S12.

3.2. Overall Reaction Chemistry. Considering the degradation reaction schemes presented in Figures 1 and 2, the overall degradation reactions of 1–5 are considered for AMP and A2P degradation.



In a CO_2 -loaded aqueous solution blend of A2P–AMP, the rate equation for DMOZD formation can be written as

rate of DMOZD formation

$$= k_1 [\text{AMP}]^a [\text{CO}_2]^b (1 + k_2 [\text{A2P}]^c) \quad (6)$$

where k_i are rate constants and defined as eq 7

$$k_i = k_{0i} e^{-E_a/RT} \quad (7)$$

At the initial rate conditions

$$d[\text{DMOZD}]/dt|_{t=0} = -d[\text{AMP}]/dt|_{t=0}$$

where k_0 , E_a , R , T , $[\text{AMP}]$, $[\text{A2P}]$, and $[\text{CO}_2]$ are the pre-exponential factor, activation energy, gas constant, temperature in Kelvin, and AMP, A2P, and CO_2 concentrations in mol/L, respectively. To be consistent with previous work, in eq 6 for the CO_2 concentration, the same unit as AMP and A2P is considered in mol/L. However, for the simplicity and ease of use in the case of A2P degradation rate equations, the CO_2 loading unit of $\text{mol}_{\text{CO}_2}/\text{mol}_{\text{AMP}+\text{A2P}}$ will be used instead of its concentration in molarity, as can be seen in eq 8

rate of A2P degradation

$$= k_1 e^{-E_a/RT} [\text{A2P}]^a [\text{CO}_{2,\text{Ld}}]^b (1 + k_2 [\text{AMP}]^c) \quad (8)$$

where k_1 , k_2 , $[\text{AMP}]$, and $[\text{A2P}]$ have the same definition as mentioned above, except for $[\text{CO}_{2,\text{Ld}}]$, the solution loading in the unit of $\text{mol}_{\text{CO}_2}/\text{mol}_{\text{AMP}+\text{A2P}}$ will be used, instead of mol/L, for the CO_2 concentration. Parameters a , b , and c are reaction orders corresponding to reaction components. To employ eqs 6 and 8, the experimental rate data are used to estimate the initial rates from concentration–time data in Figures 3–6, and S1–S12.

The rate parameters for the DMOZD formation rate, eq 6, in aqueous solutions of AMP were reported in previous work, and are slightly tuned in this study according to the experimental rate data for the AMP–A2P blend.³⁷ Therefore, in eqs 6 and 7, parameters c and k_0 need to be determined. In some initial calculations, the method for isolating compounds

Table 2. AMP–A2P Blend Thermal Degradation Kinetic Parameters for Eq 6

	eq 6—AMP	eq 8—A2P
$k_{01}/[(\text{mol/L})^{(1-a-b)} \text{s}^{-1}]$	$1.61 \times 10^9 (\pm 0.21 \times 10^9)$	$1.35 \times 10^7 (\pm 0.13 \times 10^7)$
$k_{02}/[(\text{mol/L})^{(1-a-b-c)} \text{s}^{-1}]$	$1.70 \times 10^3 (\pm 0.43 \times 10^3)$	$1.35 \times 10^2 (\pm 0.76 \times 10^2)$
$E_{a1}/[\text{kJ/mol}]$	$133.23 (\pm 6.64)$	$110.10 (\pm 5.71)$
$E_{a2}/[\text{kJ/mol}]$	$98.33 (\pm 8.55)$	$84.93 (\pm 6.32)$
a	$1.35 (\pm 0.11)$	$1.60 (\pm 0.10)$
b	$0.77 (\pm 0.08)$	$1.12 (\pm 0.17)$
c	$0.13 (\pm 0.07)$	$0.14 (\pm 0.09)$

with high concentration was utilized to estimate the starting values for reaction parameters. However, this approach was not critical in parameter estimation. Parameters including k_0 , E_a , a , b , and c (Table 2) were calculated using the nonlinear regression analysis function in Microsoft Excel.

Equations 6 and 8 can be expressed as eq 9

rate (DMOZD formation or A2P degradation)

$$= R1 \times (1 + R2) \quad (9)$$

Applying the rate parameters introduced in Table 2, the R1 (AMP) and R2 (A2P) values can be calculated. In this way, in either case of eqs 6 or 8 in all of the ranges of investigated solution concentrations, loadings, and temperatures, the R1 values are about 2 orders of magnitude higher than R2 (i.e., $R2 \ll R1$), and the R1 values are about 8 orders of magnitude higher than $R1 \times R2$, which confirms the relatively independent degradation rate of both amines with respect to the presence of the other one in the solution.

Figures 7–9 show the DMOZD formation rate as a function of AMP, A2P, and CO₂ concentrations. The rate equation

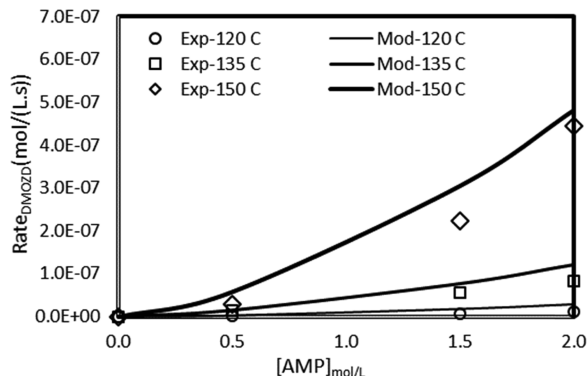


Figure 7. Model prediction using eq 6, evaluated against the experimental rate data and AMP concentration ($[A2P] = 3.5 \text{ M}$, and CO_2 loading around $0.6 \text{ mol}_{\text{CO}_2}/\text{mol}_{\text{AMP}+\text{A2P}}$).

predicts the effect of AMP concentration on the DMOZD formation rate in an acceptable range, Figure 7. It can be seen that at low temperatures, AMP concentration changes do not have a significant impact on the DMOZD formation rate. However, at the highest experimental temperature, just by increasing the AMP concentration (0.5 M), the rate of DMOZD formation is increased by a factor of 2. As shown in Figure 8, the experimental rate data display a relatively flat line and close to independent values with respect to A2P concentration in the solution. However, the rate model presents a slight slope, regardless of the description that $R2 \ll R1$, especially at high temperature. Because of the lower value of R2 with respect to R1, in terms of eq 6 parameters

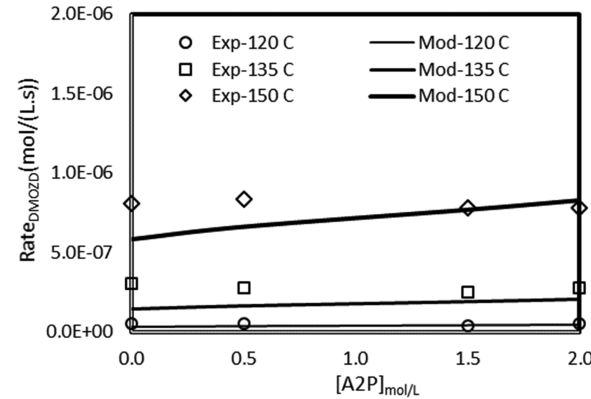


Figure 8. Model prediction using eq 6, evaluated against the experimental rate data and A2P concentration ($[A2P] = 3.5 \text{ M}$, and CO_2 loading around $0.6 \text{ mol}_{\text{CO}_2}/\text{mol}_{\text{AMP}+\text{A2P}}$).

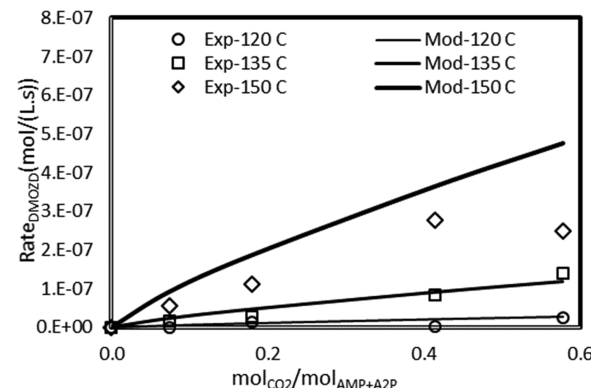


Figure 9. Model prediction using eq 6, evaluated against the experimental rate data and CO_2 loading ($[A2P] = [A2P] = 2.5 \text{ M}$).

tabulated in Table 2, the model is less sensitive to the parameters included in the R2 part of the rate equation, i.e., c , k_{02} , and E_{a2} . However, R2 has its overall impact on the reaction rate, especially at high temperatures. Figure 9 displays the CO₂ loading effect on the reaction rate, and the model prediction ability compared to the experimental data. The model shows some deviation from the experimental values at high temperature, 150 °C, and high loadings. The experimental rate data are listed in Table S1, Supporting Information.

The temperature-dependent reaction rate constants, k_1 and k_2 calculated for eq 6, vary from $3.3 \times 10^{-9} (\text{mol/L})^{(1-a-b)} \text{s}^{-1}$ at 120 °C to $5.9 \times 10^{-8} (\text{mol/L})^{(1-a-b)} \text{s}^{-1}$ at 150 °C for k_1 and $1.5 \times 10^{-10} (\text{mol/L})^{(1-a-b-c)} \text{s}^{-1}$ at 120 °C to $1.2 \times 10^{-9} (\text{mol/L})^{(1-a-b-c)} \text{s}^{-1}$ at 150 °C for k_2 . Table 3 displays the reported literature value for various amine degradation rate constants compared to this work. It should be noted that the rate equations employed in the literature represented in Table

Table 3. AMP Thermal Degradation Rate Constant Compared to the Other Amines and Literature Values

solvent	concentration	CO_2 loading ($\text{mol}_{\text{CO}_2}/\text{mol}_{\text{amine}}$)	$k/10^{-9}$	$k/10^{-9}$	references
AMP	1.12–3.36 ^a	0.17–0.7	68.2 ^d	263.0 ^d	32
AMP–A2P blend	0.5–3.5 ^a	0.07–0.67 ^c	14.7 ^e	59.1 ^e	this work
			0.44 ^f	1.24 ^f	
AMP	7 ^b	0.4	21 ^g	86 ^g	14, 16
MEA	7 ^b	0.4	134 ^g	807 ^g	14, 16
PZ	8 ^b	0.3	1.2 ^g	6.1 ^g	14, 16

^aM = molarity (for the AMP–A2P blend shows each amine concentration). ^bm = molality. ^c $\text{mol}_{\text{CO}_2}/\text{mol}_{\text{AMP}+\text{A2P}}$. ^d($\text{mol}/\text{L})^{(1-a-b)}$ s^{-1} . ^eFirst rate constant, k_1 , in eq 6, ($\text{mol}/\text{L})^{(1-a-b)}$ s^{-1} . ^fSecond rate constant, k_2 , in eq 6, ($\text{mol}/\text{L})^{(1-a-b-c)}$ s^{-1} . ^g s^{-1} .

3 are in various forms in terms of their dependency on different components in the solution. However, the first reaction rate constant, k_1 , in eq 6 obtained in this study, as 14.7×10^{-9} ($\text{mol}/\text{L})^{(1-a-b)}$ s^{-1} at 135 °C and 59.1×10^{-9} ($\text{mol}/\text{L})^{(1-a-b)}$ s^{-1} at 150 °C, compared to its corresponding value from our previous work in a single AMP system, i.e., 68.2×10^{-9} ($\text{mol}/\text{L})^{(1-a-b)}$ s^{-1} at 135 °C and 263.0×10^{-9} ($\text{mol}/\text{L})^{(1-a-b)}$ s^{-1} at 150 °C shows a descending trend by a factor around 4.5 for k_1 . This discrepancy reveals the impact of a small change in activation energy on the overall reaction rate because of the blended nature of the AMP–A2P solvent. Therefore, while A2P does not have a significant impact on the rate change of AMP degradation to DMOZD, the presence of A2P might have some type of retarding effect on AMP degradation by increasing the activation energy of reaction 1. According to the rate parameter values compared to the previous work along with other changes in the rest of the parameters, the E_{a1} shows the high impact that has been changed from 129.12 to 133.22 kJ/mol, in this work, Table 2.³² Assuming we are close to a global minimum of the objective function for rate model, and the obtained parameters are reliable, this insignificant increase in activation energy for the R1 increases the energy barrier for AMP degradation to DMOZD through R1 pathway. However, the R2 term in the rate eq 9 compensates this decrease in the degradation rate in the blend by a parallel and apparent intermolecular reaction, which again slightly increases the DMOZD formation. Therefore, in total, there is no noticeable change in DMOZD overall rate of formation.

The A2P degradation rate versus AMP, A2P, and CO_2 concentrations, is displayed in Figures 10–12. In terms of the

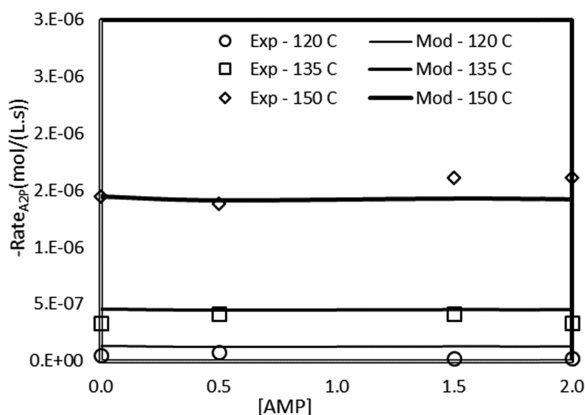


Figure 10. Model prediction, eq 8, compared to the experimental rate data as a function of AMP concentration, [A2P] = 3.5 M, and CO_2 loading around 0.60 (± 0.01) $\text{mol}_{\text{CO}_2}/\text{mol}_{\text{AMP}+\text{A2P}}$.

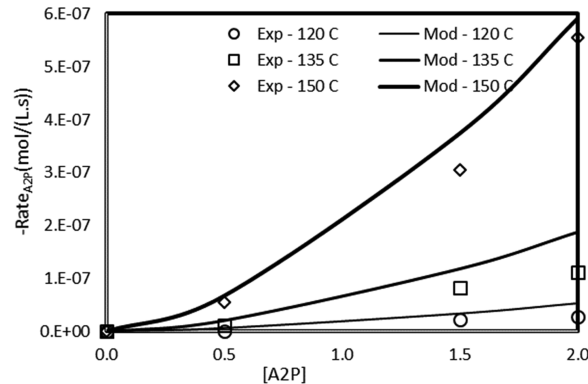


Figure 11. Model prediction, eq 8, evaluated against/in comparison to the experimental rate data versus A2P concentration, $[\text{AMP}] = 3.5$ M, and CO_2 loading around 0.60 (± 0.01) $\text{mol}_{\text{CO}_2}/\text{mol}_{\text{AMP}+\text{A2P}}$.

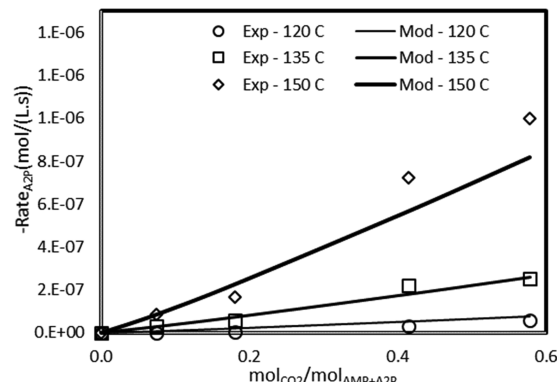


Figure 12. Model prediction, eq 8, compared to the experimental rate data versus CO_2 loading, $[\text{AMP}] = [\text{A2P}] = 2.5$ M.

A2P degradation rate as a function of another amine in the solution, i.e., AMP concentrations, the model eq 8, provides better prediction than DMOZD case, Figures 9 and 10. The model predicts a consistent trend with the experimental data and no noticeable change in the A2P degradation rate when changing the AMP concentration in the blend solution. On the other hand, the A2P degradation, as expected, increases with the A2P concentration and also CO_2 loading in the solution, Figures 11 and 12. To obtain a better match between the model prediction ability with experimental values at high temperatures, it was a tradeoff between the loading and A2P concentration effects to find a middle point to estimate both at a reasonable agreement, Figures 11 and 12 at 150 °C. However, considering the rate parameters and solution composition at various temperatures, Table 1 and S1–S3,

and eqs 6 and 8, the rate models present a 3.16 times increase in the A2P degradation rate with a 15 °C increase in solution temperature, compared to 4.02 in the case of the DMOZD formation rate. This presents a slightly higher effect of temperature on AMP degradation than A2P.

As can be seen in Figures 13, 14, and Table 2, the activation energy for the R2 term in either the case of DMOZD

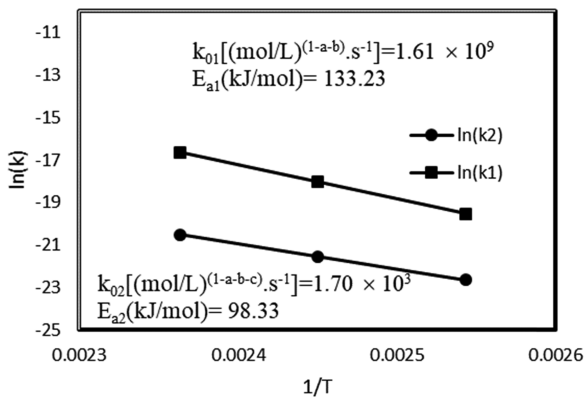


Figure 13. Natural logarithm of rate constants as a function of inverse temperature ($1/T$) with the estimated activation energy and pre-exponential factor and for eq 6.

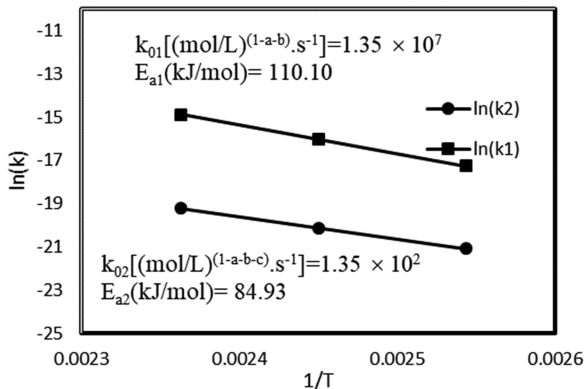


Figure 14. Natural logarithm of rate constants as a function of inverse temperature ($1/T$) with the estimated activation energy and pre-exponential factor and for eq 8.

formation or A2P degradation rates is lower than R1 terms, which represents the low energy barrier for the degradation reactions through third component involvement. However, the orders of magnitude lower pre-exponential factor values of R2 terms compared to the R1 holds the degradation reactions away from the third molecule involvement.

4. CONCLUSIONS

The A2P and AMP initial degradation rates in their CO₂-loaded aqueous solution blend were investigated. The experimental kinetic data were obtained for the blend solution degradation to obtain the rate equations. The rate data were based on the initial rate estimation for alkanolamines. In the case of AMP degradation, the DMOZD formation rate as a sole product was considered equivalent to the AMP degradation rate, particularly at the experimental conditions in this work. In terms of A2P, at the experimental conditions in this work, it showed various degradation products, some in parallel reactions, eqs 2–5. Therefore, the same assumption as

AMP to DMOZD is not reasonable for A2P, and its total degradation was considered as the rate of A2P disappearance in the reaction medium. The degradation rates for either AMP or A2P presents very low sensitivity to the concentration of other alkanolamine in the solution. The comparison of AMP degradation to DMOZD in its single amine solutions with the results from this study revealed a very slight effect of blend solution on the degradation rate. The rate models for both AMP and A2P degradations showed an insignificant effect of the amines on each other in terms of their conversion rate to degradation products. The activation energies obtained for the apparent reactions involved three molecules (A2P, AMP, and CO₂), i.e., R2 term in the reaction equations, presented lower values with the orders of magnitude higher pre-exponential factors, which lead to a lower chance for the reaction through a third component. Therefore, at least in the system studied in this work during the initial degradation period, the presence of the second alkanolamine in the solution does not have a significant impact on the other alkanolamine's degradation.

ASSOCIATED CONTENT

S Supporting Information

The Supporting Information is available free of charge at <https://pubs.acs.org/doi/10.1021/acs.iecr.9b05364>.

DMOZD concentration versus time at 120, 135, and 150 °C at different A2P and AMP concentrations and CO₂ loadings (Figures S1–S6); A2P concentration as a function of time at 120, 135, and 150 °C at different AMP concentrations and CO₂ loadings (Figures S7–S12); experimental kinetic data (Table S1) (PDF)

AUTHOR INFORMATION

Corresponding Author

*E-mail: kunlei.liu@uky.edu.

ORCID

Kunlei Liu: [0000-0003-3229-0260](https://orcid.org/0000-0003-3229-0260)

Notes

The authors declare no competing financial interest.

ACKNOWLEDGMENTS

The authors acknowledge the Carbon Management Research Group (CMRG) members, including Louisville Gas & Electric (LG&E) and Kentucky Utilities (KU), Duke Energy, and Electric Power Research Institute (EPRI) for their financial support.

REFERENCES

- Chen, P.-C.; Yang, M.-W.; Wei, C.-H.; Lin, S. Z. Selection of blended amine for CO₂ capture in a packed bed scrubber using the Taguchi method. *Int. J. Greenhouse Gas Control* 2016, 45, 245–252.
- Kim, S.; Shi, H.; Lee, J. Y. CO₂ absorption mechanism in amine solvents and enhancement of CO₂ capture capability in blended amine solvent. *Int. J. Greenhouse Gas Control* 2016, 45, 181–188.
- Sakwattanapong, R.; Aroonwilas, A.; Veawab, A. *Kinetics of CO₂ Capture by Blended MEA-AMP*, 2006 IEEE EIC Climate Change Conference, 10–12 May 2006; pp 1–6.
- Silkenbäumer, D.; Rumpf, B.; Lichtenthaler, R. N. Solubility of Carbon Dioxide in Aqueous Solutions of 2-Amino-2-methyl-1-propanol and N-Methyldiethanolamine and Their Mixtures in the Temperature Range from 313 to 353 K and Pressures up to 2.7 MPa. *Ind. Eng. Chem. Res.* 1998, 37, 3133–3141.

- (5) Dash, S. K.; Samanta, A. N.; Bandyopadhyay, S. S. Solubility of carbon dioxide in aqueous solution of 2-amino-2-methyl-1-propanol and piperazine. *Fluid Phase Equilib.* **2011**, *307*, 166–174.
- (6) Bougie, F.; Iliuta, M. C. CO₂ Absorption into Mixed Aqueous Solutions of 2-Amino-2-hydroxymethyl-1,3-propanediol and Piperazine. *Ind. Eng. Chem. Res.* **2010**, *49*, 1150–1159.
- (7) Park, S. H.; Lee, K. B.; Hyun, J. C.; Kim, S. H. Correlation and Prediction of the Solubility of Carbon Dioxide in Aqueous Alkanolamine and Mixed Alkanolamine Solutions. *Ind. Eng. Chem. Res.* **2002**, *41*, 1658–1665.
- (8) Chung, P.-Y.; Soriano, A. N.; Leron, R. B.; Li, M.-H. Equilibrium solubility of carbon dioxide in the amine solvent system of (triethanolamine+piperazine+water). *J. Chem. Thermodyn.* **2010**, *42*, 802–807.
- (9) Yang, Z.-Y.; Soriano, A. N.; Caparanga, A. R.; Li, M.-H. Equilibrium solubility of carbon dioxide in (2-amino-2-methyl-1-propanol+piperazine+water). *J. Chem. Thermodyn.* **2010**, *42*, 659–665.
- (10) Derk, P. W. J.; Hogendoorn, J. A.; Versteeg, G. F. Experimental and theoretical study of the solubility of carbon dioxide in aqueous blends of piperazine and N-methyldiethanolamine. *J. Chem. Thermodyn.* **2010**, *42*, 151–163.
- (11) Ai, N.; Chen, J.; Fei, W. Solubility of Carbon Dioxide in Four Mixed Solvents. *J. Chem. Eng. Data* **2005**, *50*, 492–496.
- (12) Haghtalab, A.; Izadi, A. Simultaneous measurement solubility of carbon dioxide+hydrogen sulfide into aqueous blends of alkanolamines at high pressure. *Fluid Phase Equilib.* **2014**, *375*, 181–190.
- (13) Li, H.; Frailie, P. T.; Rochelle, G. T.; Chen, J. Thermodynamic modeling of piperazine/2-aminomethylpropanol/CO₂/water. *Chem. Eng. Sci.* **2014**, *117*, 331–341.
- (14) Lin, P.-H.; Wong, D. S. H. Carbon dioxide capture and regeneration with amine/alcohol/water blends. *Int. J. Greenhouse Gas Control* **2014**, *26*, 69–75.
- (15) Naami, A.; Sema, T.; Edali, M.; Liang, Z.; Idem, R.; Tontiwachwuthikul, P. Analysis and predictive correlation of mass transfer coefficient KGav of blended MDEA-MEA for use in post-combustion CO₂ capture. *Int. J. Greenhouse Gas Control* **2013**, *19*, 3–12.
- (16) Mudhasakul, S.; Ku, H.-M.; Douglas, P. L. A simulation model of a CO₂ absorption process with methyldiethanolamine solvent and piperazine as an activator. *Int. J. Greenhouse Gas Control* **2013**, *15*, 134–141.
- (17) Pinto, D. D. D.; Monteiro, J. G. M. S.; Bersås, A.; Haug-Warberg, T.; Svendsen, H. F. eNRTL Parameter Fitting Procedure for Blended Amine Systems: MDEA-PZ Case Study. *Energy Procedia* **2013**, *37*, 1613–1620.
- (18) Hartono, A.; Saeed, M.; Ciftja, A. F.; Svendsen, H. F. Modeling of Binary and Ternary VLE of the AMP/Pz/H₂O System. *Energy Procedia* **2013**, *37*, 1736–1743.
- (19) Kundu, M.; Bandyopadhyay, S. S. Solubility of CO₂ in Water + Diethanolamine + 2-Amino-2-methyl-1-propanol. *J. Chem. Eng. Data* **2006**, *51*, 398–405.
- (20) Wu, S.-H.; Caparanga, A. R.; Leron, R. B.; Li, M.-H. Vapor pressures of aqueous blended-amine solutions containing (TEA/AMP/MDEA)+(DEA/MEA/PZ) at temperatures (303.15–343.15)K. *Exp. Therm. Fluid Sci.* **2013**, *48*, 1–7.
- (21) Shi, H.; Naami, A.; Idem, R.; Tontiwachwuthikul, P. 1D NMR Analysis of a Quaternary MEA–DEAB–CO₂–H₂O Amine System: Liquid Phase Speciation and Vapor–Liquid Equilibria at CO₂ Absorption and Solvent Regeneration Conditions. *Ind. Eng. Chem. Res.* **2014**, *53*, 8577–8591.
- (22) Rebolledo-Libreros, M.; Trejo, A. Gas solubility of CO₂ in aqueous solutions of N-methyldiethanolamine and diethanolamine with 2-amino-2-methyl-1-propanol. *Fluid Phase Equilib.* **2004**, *218*, 261–267.
- (23) Zhao, Y.; Winston Ho, W. S. Steric hindrance effect on amine demonstrated in solid polymer membranes for CO₂ transport. *J. Membr. Sci.* **2012**, *415–416*, 132–138.
- (24) Ciftja, A. F.; Hartono, A.; da Silva, E. F.; Svendsen, H. F. Study on carbamate stability in the Amp/CO₂/H₂O system from ¹³C-NMR spectroscopy. *Energy Procedia* **2011**, *4*, 614–620.
- (25) Yih, S. M.; Shen, K. P. Kinetics of carbon dioxide reaction with sterically hindered 2-amino-2-methyl-1-propanol aqueous solutions. *Ind. Eng. Chem. Res.* **1988**, *27*, 2237–2241.
- (26) Eustaquier-Rincón, R.; Rebolledo-Libreros, M. E.; Trejo, A.; Molnar, R. Corrosion in Aqueous Solution of Two Alkanolamines with CO₂ and H₂S: N-Methyldiethanolamine + Diethanolamine at 393 K. *Ind. Eng. Chem. Res.* **2008**, *47*, 4726–4735.
- (27) Mimura, T.; Shimojo, S.; Suda, T.; Iijima, M.; Mitsuoka, S. Research and development on energy saving technology for flue gas carbon dioxide recovery and steam system in power plant. *Energy Convers. Manage.* **1995**, *36*, 397–400.
- (28) Mahajani, V. V.; Joshi, J. B. Kinetics of reactions between carbon dioxide and alkanolamines. *Gas Sep. Purif.* **1988**, *2*, 50–64.
- (29) Águila-Hernández, J.; Trejo, A.; García-Flores, B. E. Surface tension and foam behaviour of aqueous solutions of blends of three alkanolamines, as a function of temperature. *Colloids Surf., A* **2007**, *308*, 33–46.
- (30) Alvarez, E.; Cancela, Á.; Maceiras, R.; Navaza, J. M.; Táboas, R. Surface Tension of Aqueous Binary Mixtures of 1-Amino-2-Propanol and 3-Amino-1-Propanol, and Aqueous Ternary Mixtures of These Amines with Diethanolamine, Triethanolamine, and 2-Amino-2-methyl-1-propanol from (298.15 to 323.15) K. *J. Chem. Eng. Data* **2003**, *48*, 32–35.
- (31) Mazari, S. A.; Ali, B. S.; Jan, B. M.; Saeed, I. M. Thermal degradation of piperazine and diethanolamine blend for CO₂ capture. *Int. J. Greenhouse Gas Control* **2016**, *47*, 1–7.
- (32) Matin, N. S.; Thompson, J.; Onnweeer, F. M.; Liu, K. Thermal Degradation Rate of 2-Amino-2-methyl-1-propanol to Cyclic 4,4-Dimethyl-1,3-oxazolidin-2-one: Experiments and Kinetics Modeling. *Ind. Eng. Chem. Res.* **2016**, *55*, 9586–9593.
- (33) Wang, T.; Jens, K.-J. Oxidative Degradation of Aqueous 2-Amino-2-methyl-1-propanol Solvent for Postcombustion CO₂ Capture. *Ind. Eng. Chem. Res.* **2012**, *51*, 6529–6536.
- (34) Stowe, H. M.; Vilčiukas, L.; Paek, E.; Hwang, G. S. On the origin of preferred bicarbonate production from carbon dioxide (CO₂) capture in aqueous 2-amino-2-methyl-1-propanol (AMP). *Phys. Chem. Chem. Phys.* **2015**, *17*, 29184–29192.
- (35) Zheng, L.; Matin, N. S.; Thompson, J.; Landon, J.; Holubowitch, N. E.; Liu, K. Understanding the corrosion of CO₂-loaded 2-amino-2-methyl-1-propanol solutions assisted by thermodynamic modeling. *Int. J. Greenhouse Gas Control* **2016**, *54*, 211–218.
- (36) Matin, N. S.; Thompson, J.; Onnweeer, F. M.; Liu, K. Thermal Degradation Rate of 2-Amino-2-methyl-1-propanol to Cyclic 4,4-Dimethyl-1,3-oxazolidin-2-one; Mechanistic Aspects and Kinetics Investigation. *Ind. Eng. Chem. Res.* **2017**, *56*, 9437–9445.
- (37) Matin, N. S.; Thompson, J.; Onnweeer, F. M.; Liu, K. Thermal Degradation Rate of 2-Amino-2-methyl-1-propanol to Cyclic 4,4-Dimethyl-1,3-oxazolidin-2-one: Experiments and Kinetics Modeling. *Ind. Eng. Chem. Res.* **2016**, *55*, 9586–9593.
- (38) Thompson, J. G.; Bhatnagar, S.; Combs, M.; Abad, K.; Onnweeer, F.; Pelgen, J.; Link, D.; Figueroa, J.; Nikolic, H.; Liu, K. Pilot testing of a heat integrated 0.7MWe CO₂ capture system with two-stage air-stripping: Amine degradation and metal accumulation. *Int. J. Greenhouse Gas Control* **2017**, *64*, 23–33.
- (39) da Silva, E. F.; Lepaumier, H.; Grimstvedt, A.; Vevelstad, S. J.; Einbu, A.; Vernstad, K.; Svendsen, H. F.; Zahlsen, K. Understanding 2-Ethanolamine Degradation in Postcombustion CO₂ Capture. *Ind. Eng. Chem. Res.* **2012**, *51*, 13329–13338.
- (40) Gouédard, C. Novel degradation products of ethanolamine (MEA) in CO₂ capture conditions: identification, mechanisms proposal and transposition to other amines. Doctoral Dissertation, Université Pierre et Marie Curie-Paris VI, 2014.